Shape and material characteristics of the trachea in the leatherback sea turtle promote progressive collapse and reinflation during dives

Colm Murphy[1], Denis Kelliher[1*], John Davenport[2]

[1]Department of Civil and Environmental Engineering, University College Cork, College Road, Cork, Ireland

[2]School of Biological, Earth and Environmental Sciences and Environmental Research Institute, University College Cork, Distillery Fields, North Mall, Cork, Ireland

*Author for correspondence (email: d.kelliher@ucc.ie)

SUMMARY

The leatherback turtle regularly undertakes deep dives and has been recorded attaining depths in excess of 1,200 m. Its trachea is an almost solid, elliptical-section tube of uncalcified hyaline cartilage with minimal connective tissue between successive rings. The structure appears to be advantageous for diving and perfectly designed for withstanding repeated collapse and reinflation. This study applies Boyle's law to the respiratory system (lungs, trachea and larynx) and estimates the changes in tracheal volume during a dive. These changes are subsequently compared with the results predicted by a corresponding finite element (FE) structural model, itself based on laboratory studies of the trachea of an adult turtle. Boyle's law predicts that the lungs will collapse first during the initial stages of dive with tracheal compression beginning at much deeper depths after complete air mass expulsion from the lungs. The FE model reproduces the changes extremely well (agreeing closely with Boyle's law estimations) and provides visual representation of the deformed tracheal luminal area. Initially, the trachea compresses both ventrally and dorsally before levelling ventrally. Bulges are subsequently formed laterally and become more pronounced at deeper depths. The geometric configuration of the tracheal structure confers both homogeneity and strength upon it, which makes it extremely suited for enduring repeated collapse and re-expansion. The structure actually promotes collapse and is an adaptation to the turtle's natural environment in which large numbers of deep dives are performed annually.

Key words: leatherback turtle, *Dermochelys*, trachea, Boyle's law, diving, shape changes

SHORT TITLE

Leatherback trachea promotes collapse

INTRODUCTION

In terms of the respiratory system, all air-breathing vertebrate lineages have been constrained by the nature of structures evolved primarily for a terrestrial existence. These consist of lungs of varying degrees of complexity, plus the upper respiratory system: the larynx and the trachea, together with bronchi that connect the trachea to the lungs (in some groups via a branching bronchial tree). Lungs have little resistance to compression, while the tracheae and bronchi of terrestrial reptiles, birds and mammals have a common structure designed to maintain a patent airway, yet provide flexibility, especially in the neck region. They are all composed of a series of circular, semi-rigid cartilaginous rings (complete in some groups, incomplete in others), interspersed with sections of thin and stretchable connective tissue.

Diving air-breathing vertebrates encounter a number of problems that are exacerbated by increasing depth and duration of dives (Kooyman, 1989). First, they require adequate oxygen supplies for each dive, but all diving groups feature enhanced blood and tissue storage of oxygen, and generally have rather smaller lungs than do related groups of terrestrial vertebrates. Second, the air spaces of the respiratory system become compressed and this decreases the buoyancy of the animal concerned, increasing locomotory costs. Third, the possibility of highly compressed air being in close proximity to moving blood has the potential for causing N_2 accumulation and-decompression sickness (DCS). Scholander (1940) developed a simple 'balloon and pipe' model that addressed the DCS problem. He envisaged that the rib cage and lungs of a diving mammal would be compressed, and the latter finally collapse, at relatively shallow depths (30-50 m), displacing air into the rigid (and poorly vascularised) tubes of the upper respiratory system, where little gaseous exchange would be possible and the threat of DCS eliminated. In support of this concept, it was observed that the tracheae of diving mammals tended to have much wider tracheal rings, with far less connective tissue between them than terrestrial mammals, and that the rings were composed of more rigid materials, sometimes calcified.

In the subsequent 70 years this model has become extensively modified as understanding of the complexity of diving physiology and biochemistry has improved. Some very deep divers (e.g. Weddell seals, *Leptonychotes weddellii,* and northern elephant seals, *Mirounga angustirostris*) exhale before they dive to minimise lung volume and nitrogen accumulation (LeBoeuf et al., 1986; Ponganis et al., 1993; Sato et al., 2003), while king penguins (*Aptenodytes patagonicus*) and sperm whales (*Physeter macrocephalus*) inhale before diving (Sato et al., 2002; Miller et al., 2004), presumably to maintain buoyancy and

delay alveolar collapse to greater depths. Evidence indicates that lung collapse and gaseous exchange can be delayed to depths of well over 100 m in some seals (Kooyman and Sinnett, 1982; Moore et al., 2011b). A recent comprehensive review (Hooker et al., 2011) argues that diving mammals "manage DCS" rather than eliminate it. Whereas several shallow divers (e.g. marine otters and extinct mosasaurs) feature calcified tracheal rings that help to provide the rigid pipes envisaged by Scholander (1940), this appears not to be the case in deep divers such as Weddell seals and northern elephant seals (both of which exceed 1000 m depth on many dives). They show reduced tracheal volume when compressed in hyperbaric chambers (Kooyman et al., 1970), and it is now clear that this is caused by 'slipping' of overlapping cartilaginous rings (Moore et al., 2011a). Bostrom et al. (2008) demonstrated that a compliant trachea causes increased depth of alveolar collapse and a gradual rather than abrupt collapse.

Our study considers the structure of the leatherback sea turtle, *Dermochelys coriacea* (Vandelli 1761). Dermochelyidae diverged from other chelonians 100-150 million years ago (mya; Wood et al., 1996), so the leatherback turtle can be regarded as the living deep-diving vertebrate with the longest evolutionary history. Adult leatherbacks are large animals, typically weighing in the range of 300-500 kg but are less than 916 kg (Eckert and Luginbuhl, 1988), and overlap in size with many marine pinniped and cetacean species.

The leatherback has an unusual feeding ecology, biogeography and physiology (see Davenport et al., 2009b for review). Adult *Dermochelys* are accomplished deep divers. Diving beyond 1000 m was first inferred (Eckert et al., 1986; Eckert et al., 1989) and subsequently confirmed by satellite tags (Houghton et al., 2008). Maximum recorded dive depths and dive durations have now been extend to 1280 m (Doyle et al., 2008) and 86.5 min (López-Mendilaharsu et al., 2009), respectively. However, it is has recently been determined from satellite telemetry that very deep dives (>300 m) are rare (Houghton et al., 2008), making up only 0.4% of all dives, and exceed calculated aerobic scope for the species. Leatherbacks are mostly (99.6%) limited to aerobic dives of <300 m, but they conduct thousands of dives per year, so there are appreciable total annual numbers of very deep dives.

Dermochelys is a most unusual chelonian anatomically, with a highly modified and reduced shell structure (no bony elements protect the belly) that, with the thick leathery skin, allows the animals to vary their shape considerably (Davenport et al., 2011). Spotila (2004) reported that the ventral surface of the leatherback becomes visibly concave when leatherbacks start dives, which is consistent with respiratory tract collapse. The turtle therefore shows convergent features with marine mammals and differs considerably from the hard-shelled marine turtles which cannot reach such great depths. The anatomy of the

leatherback trachea has attracted recent anatomical study (Davenport et al., 2009b; Fraher et al., 2010). It may be seen that, as in other reptiles, the larynx and the tracheal structure begins at the anterior of the floor of the mouth (Fig. 4 in Davenport et al., 2009a). The larynx has a rectangular cross section and is thick-walled. At the rear of the hyoid plate (Fraher et al., 2010) it joins the trachea, which is a continuous long tube, consisting of fused, irregularly shaped, tracheal rings, with minimal amounts of connective tissue between them (Davenport et al., 2009b). The cross section of the trachea (Fig. 2 in Davenport et al., 2009b) is near-elliptical in shape, but thinner-walled dorsally than ventrally. The material of this nearly-elliptical tube is predominantly uninterrupted, uncalcified cartilage, with a thin vascular lining. Davenport et al. (2009b) reported that the trachea could easily be compressed between the fingers, suggesting that it should collapse progressively given small pressure differences between lumen and exterior.

The first aim of our study was to investigate the mechanical properties of the leatherback trachea. Such study has rarely been performed on tracheae of marine vertebrates, though Cozzi et al. (2005) and Bagnoli et al. (2011) made limited measurements on sections of the tracheae of the striped dolphin (*Stenella coeruleoalba)* and the bottlenose dolphin (*Tursiops truncatus*). We investigated the forces required to cause tracheal deformation in the laboratory and used the data recorded to investigate material behaviour. We also studied the hysteresis properties of the tracheal material, since diving and surfacing take place thousands of times per year. The second aim of the study was to examine the likely changes in the tracheal volume (expressed as changes in the luminal area) during the diving process through a simplified application of Boyle's law and to model these changes in a finite element (FE) structural model. In doing so we were aware that most previous considerations of tracheal behaviour have treated the trachea as an isolated structure. However, from previously published figures (Fig. 4 in Davenport et al., 2009a; Fig. 2 in Davenport et al., 2009b) it may be seen that the forepart of the trachea is surrounded by tissue (mostly muscle and blubber), to which it is connected. Only when it emerges posteriorly from the neck (which has low mobility in this species) into the general body cavity (sea turtles do not have separate thoracic and abdominal cavities) does it become less constrained, and even then is bound to the dorsal wall of that cavity. We have therefore taken into account the surrounding tissues in our modelling. In addition, while it is possible to model the behaviour of the trachea assuming a fixed mass of air within it, we have also taken into account the dynamic situation of real dives, during which air from the collapsing lungs moves into the upper respiratory tract and so serves to keep the trachea inflated to greater depths (Bostrom et al., 2008). A recent paper

(Fossette et al., 2010) has demonstrated that *Dermochelys* inspires before diving and proposes that this is primarily concerned with buoyancy regulation. However, this inspiration will also delay lung collapse to greater depths. Our calculations in the application of Boyle's law rely on the estimates of leatherback lung volume made by Lutcavage et al. (1992).

MATERIALS AND METHODS

Material testing

Tracheal cartilage samples for material testing were obtained from a freshly stranded adult female leatherback turtle at Ballycotten, East Cork, Ireland (see Davenport et al., 2009b for review). Non-destructive compressive testing was performed on a single tracheal portion in order to investigate the response of the material to external loadings. The portion, some 20 mm front to back, was taken from the upper region of the trachea, about 50 mm caudal to the posterior end of the larynx and well before the point of bifurcation. It was estimated that the trachea had a length of about 450 mm, based on the assumption that the material and geometric properties of the remaining tracheal portion in the disposed carcass were similar to those in the preserved material. It had a near-elliptical cross section with the following approximate measurements; external diameter 42 x 29 mm; internal diameter 33 x 23 mm; maximum dorsal thickness 2.1 mm, maximum ventral thickness 3.6 mm (Davenport et al., 2009b). The average width of the sample tested was measured to be 8.6 mm ± 0.3 mm. The sample was placed on the lower flat plat of a Tinius Olsen Benchtop Tester H5K-S UTM (Tinius Olsen Ltd., Salfords (Near Redhill), Surrey, England) and a compressive point displacement was applied to the dorsal side (Fig. 1A, B). Testing of the sample adhered to all biomechanical standards and procedures. The sample was preconditioned five times (Fung, 1993) using a compressive velocity of 5 mm min^{-1} at room temperature and a 50 N load cell (0.001 N and 0.001 mm precision), with the applied displacements and corresponding loads being recorded during all testing cycles.

Finite element modelling

The lung-trachea-larynx system is clearly a complex structural engineering problem that would be very difficult to model three-dimensionally. However, under due consideration of both the biology and physics of the system, a much simpler two-dimensional (2-D) model can capture the important responses. 2-D plane strain models assume that the structure is infinite in length so that no strain is possible in this direction. As the leatherback trachea is an almost solid tube of cartilage (Davenport et al., 2009b), and since the majority of the trachea is embedded in the musculature and fat in the neck, a 2-D plane strain slice through the neck section (capturing the tracheal luminal area) will simulate the response of the majority of the length of the trachea. It certainly will quantify, to within reasonable accuracy, the

deformation of the trachea as the whole system is subject to increasing pressure. The geometry used in the 2-D structural model is taken from Computed Tomography (CT) transverse sectional images of the head and neck of the female turtle (Fig. 4 in Davenport et al., 2009a) and was imported into the FE analysis software system Strand7 (© Copyright Strand7 Pty Ltd., Sydney, New South Wales, Australia). Included in the model were the tracheal cartilage, the surrounding soft tissues and the vertebral column (Fig. 2). The stiff vertebral column was modelled as rigid and fixed in space to provide adequate fixity for overall stability. Both the tracheal cartilage (initial luminal area 571 mm^2) and the soft tissues were modelled using separate hyper-elastic isotropic constitutive material models (described in detail in Material Behaviour). There were 9,733 degrees of freedom in the model, analysed using a mixed FE mesh of eight-node rectangular and six-node triangular isoparametric elements. The simulation of the structural response of the neck section during a dive was achieved using a nonlinear static solver. Loading conditions were based on the application of Boyle's law (see Loading conditions). The reported results of this analysis consisted of the deformed shapes and the tracheal luminal area in 5 m increments from surface level to a maximum depth of 1,500 m.

Material behaviour

Cartilage samples responded almost elastically when compressed both by human touch (Davenport et al., 2009b) and between flat plates (this study). Its behaviour resembled a rubber material in that it returned to its initial shape even after it was subjected to large deformations. Compressive testing of the material revealed that it exhibited both nonlinear (although almost linear during loading) and viscoelastic behaviour (see Results). In order to model both the nonlinear and apparent rubber-like behaviour, the cartilage has been treated as a nonlinear hyper-elastic material and the Mooney-Rivlin rubber material formulation was applied to model its behaviour in the FE simulations. The two material constants required for this constitutive model were obtained using an integrated mathematical optimisation, FE simulation and experimental testing methodology (Murphy et al., 2010). Poisson's ratio, a measure of incompressibility, was assigned a value of 0.49, which correlates well with values cited in other studies (Teng et al., 2008; Teng et al., 2009a; Teng et al., 2009b; Trabelsi et al., 2010).

Knowledge of the mechanical properties of the adjacent soft tissues (striated muscle and connective tissue) is limited. In previous studies tracheal smooth muscle has been treated as a nonlinear material using hyper-elastic constitutive material models (Begis et al., 1988; Costantino et al., 2004; Teng et al., 2009a; Teng et al., 2009b; Trabelsi et al., 2010; Bagnoli et al., 2011) with Poisson's ratio ranging from being completely incompressible (Begis et al., 1988; Teng et al., 2009a; Teng et al., 2009b) to nearly incompressible (0.475, Costantino et al., 2004). A slightly lower value was also applied in another study (0.45, Bagnoli et al., 2011). In this study all the surrounding soft tissues have been assumed to be homogeneous and are modelled as an incompressible hyper-elastic material using the generalised Mooney-Rivlin hyper-elastic material model. The constants for this constitutive model were obtained by applying the stress-strain data for smooth muscle published by Bagnoli et al. (2011).

Loading conditions

The loading conditions applied in this model are based on Boyle's law. When combined, the lungs (*LG*), the trachea (*T*) and the larynx (*LX*) may be treated as a closed system. The external hydrostatic pressure, *P*, acting on this system at depth, *x*, and the volume, *V*, of the system may be related through the constant, *k*, as stated in Boyle's law (Eqn 1):

$$PV = k \tag{1}$$

It has been shown that the compliant lungs (and alveoli) collapse early during the initial depths of a dive (Bostrom et al., 2008). In contrast to this, the trachea and the larynx are much stiffer structures: the larynx may be considered a rigid box and the trachea resembles an almost solidified tube of uncalcified cartilage (Davenport et al., 2009b). As the larynx and the trachea are sufficiently stiffer than the lungs it is therefore the case that as the lungs collapse the change in volume of the lungs with depth, $V_{LG\,x}$, (from a reference position of 0 m at surface level) may be represented by Eqn 2:

$$V_{LGx} = \frac{P_0}{P_x}\left(V_{LX\,0} + V_{T\,0} + V_{LG\,0}\right) - V_{LXx} - V_{Tx}, \tag{2}$$

where P_0 is the initial pressure at surface level, P_x is the pressure acting at depth *x*, $V_{LX\,0}$, $V_{T\,0}$ and $V_{LG\,0}$ are the volumes of the larynx, the trachea and the lungs respectively at surface level, and $V_{LX\,x}$ and $V_{T\,x}$ are the volumes of the larynx and the trachea respectively at depth *x*. It is possible that lung volume decreases with increasing depth as a result of nitrogen

absorption driven by increased partial pressure, thereby leading to reductions in the depth at which complete lung collapse occurs. However, we are unable to calculate how significant a contribution such absorption might make as no knowledge of pulmonary blood perfusion during diving is currently available. The air mass in the entire closed system is therefore deemed to remain constant during both descent and ascent. Throughout the duration of collapse residual air mass in the lungs is forced to enter the larynx and the trachea. Simple equilibrium dictates that the internal air pressure in the tracheal lumen must be equal in magnitude but opposite in direction to the external hydrostatic pressures at depth. A similar scenario may be put forward for tracheal collapse. Assuming tracheal deformation begins at the depth at which the lungs have collapsed completely (and at which there is no more air mass available to oppose external hydrostatic pressures), and that the larynx is sufficiently stiffer, the change in volume of the trachea with depth, V_{Tx}, may be represented through Eqn 3:

$$V_{Tx} = \frac{P_0}{P_x}\left(V_{LX0} + V_{T0} + V_{LG0}\right) - V_{LXx} \quad \textbf{(3)}$$

This equation may be used to estimate the tracheal luminal area at a given depth (*Volume = Area x Length*) after complete lung collapse. For the purposes of investigating the change in the area of the tracheal lumen it is assumed in Eqn 3 that changes in the tracheal length may be ignored. The same assumption was made by Bostrom et al. (2008). As the trachea is an almost tube-like structure (Davenport et al., 2009b) and connected to the very rigid larynx, it is reasonable to expect insignificant deformation axially and, therefore, the volume change in the trachea will manifest itself as a change in luminal area (in line with the 2-D FE model described in Finite element modelling). Eqn 2 and Eqn 3 were evaluated in order to obtain estimates for the changes in lung volume and luminal area respectively with depth when subjected to increasing hydrostatic pressures (density, ρ = 1000 kg m^{-3}; acceleration due to gravity, g = 9.81 m s^{-2}; atmospheric pressure, P_{ATM} = 101.325 kPa; $P_x = P_{ATM} + \rho g x$). Reductions in lung volume with depth in the FE model were modelled by the application of positive hydrostatic pressures to both the exterior surface of the neck and the internal surface of the tracheal lumen. In essence, this models the air flow from the collapsing lungs into the larynx-trachea system up to the point where the lungs are completely evacuated. Subsequent tracheal collapse was then modelled as follows. The tracheal lumen was filled with an incompressible fictitious fluid, with no shear resistance, and an appropriate coefficient of thermal expansion. Then, by applying a fictitious thermal change (negative in this case) the

volume of the fluid could be controlled to reflect the change in volume predicted by Boyle's law (Eqn 3). This approach means the volume reduction is accurately modelled. Furthermore, the fluid will allow the trachea to deform, but maintain a positive pressure on the interior of the tracheal lumen, thereby satisfying the physics of the dive.

RESULTS

Material testing

The complete load-displacement history obtained from the compressive biomechanical testing of the single tracheal tubular sample is shown in Fig. 3. Like most other biological soft tissues, tracheal cartilage displays viscoelastic properties and this may be seen through the contrasting nonlinear loading and unloading histories. Hysteresis was also evident between successive cycles. In order to obtain a meaningful, and thus accurate, representation of the behaviour of the material, preconditioning was required to reduce the hysteresis effects (Fung, 1993). Fig. 3 shows that the hysteresis becomes less noticeable with an increasing number of loading cycles. However, complete curve occlusion was not attained after applying six consecutive cycles, suggesting that some viscoelastic effects remained. For the purposes of determining the two material constants in the Mooney-Rivlin material formulation only the loading history from the sixth and final cycle was correlated with the loading history obtained from the corresponding FE model, as this best reflects the behaviour of the material recorded in the laboratory. These material constants were determined to be 6.1 MPa and 1.0 MPa respectively, and lead to a bulk modulus (a measure of resistance to uniform volumetric compression) of 690.4 MPa. The characteristic stress-strain curve was evaluated using the constants and indicates that the material is stiffer (slope of curve) in compression (negative quadrant) than in tension (Fig. 4).

Volume changes predicted by Boyle's law

For the simplified formulation, in which it is assumed that there is no volume change in either the larynx or in the trachea, the depth at which the lungs collapse completely is 871 m (Eqn 2). Most of the collapse occurs in the first 50 m of the dive with subsequent increases in depth causing the volume of the system to decrease asymptotically (Fig. 5). In the similarly simplified state envisaged for tracheal collapse, the luminal area reduces gradually with increasing depth (Eqn 3). Complete luminal collapse would theoretically occur at 3,891 m.

FE Modelling

For the first 871 m in which the lungs are collapsing, there is very little change in the cross-sectional area (and hence volume) of the trachea. The tracheal luminal air pressure, representing air mass flow from the collapsing lungs, provides resistance to the external

hydrostatic pressures and prevents premature collapse. Indeed, the percentage decrease of the luminal area, between surface level and 871 m, was measured as 1.14% and was deemed to be insignificant when considering the overall luminal area change of the trachea. The assumptions made with the simplified system were therefore considered to have been modelled sufficiently. Tracheal collapse, beginning at 871 m, is progressive with both the dorsal and ventral aspects yielding as the surrounding soft tissues compress inwards (Fig. 5). The trachea subsequently levels ventrally whilst bulges are formed laterally. Additional increases in depth compress the luminal area further, making the bulges more pronounced. The integral luminal area was measured for each depth and compared with the corresponding areas predicted theoretically (Fig. 5). Good agreement was achieved at all depths (Table 1) and confirms that the model succeeded in reducing the luminal area in line with the areas predicted using the simplified application of Boyle's law. It is worth noting that a larger reduction in area is expected during early depth increments and this is captured well in the FE model results (Fig. 5).

DISCUSSION

The response of the upper airway, in particular the trachea, is an important factor when studying the physiological response of the vertebrate respiratory system in extreme pressure environments. Its deformation under external hydrostatic loadings determines the form of collapse and thus, the depth that may be attained during diving apnea. In this paper, a simplified representation of tracheal collapse based on Boyle's law was presented and a computational FE model of the behaviour of the trachea and the surrounding soft tissues based on this simplification was developed. The overall objectives of this study were to investigate how the trachea of the leatherback turtle responds during deep diving, particularly the luminal area, and to examine the importance of its structure and material properties in resisting collapse.

Boyle's law predicts that the lung volume will reduce progressively with increasing depth until complete collapse. The air mass in the lungs is, therefore, compelled to enter the trachea and the larynx, and will maintain a positive pressure on the interior wall of the tracheal lumen equal to the outside hydrostatic pressure, linearly dependant on depth. These figures rely on estimates of lung volume predicted by Lutcavage et al. (1992) and do not take into account the expected reductions in lung volume arising from the increasing partial pressures of all gases during descent. It is also assumed that air in the lungs is at capacity when diving commences (Fossette et al., 2010), and that continuity is maintained between lungs and upper airway throughout dives. For the adult turtle considered in this study, weighing 450 kg (Davenport et al., 2009b), the initial volume was calculated to be 28 litres. It is likely that leatherback body size will influence the depth at which the lungs collapse completely and changes in tracheal volume commence. However, no data for tracheal and lung sizes are currently available for a size range of *Dermochelys* that would permit further calculations. As it stands, total lung collapse (and consequent cessation of air mass flow to the trachea) is expected to occur at approximately 871 m. Tracheal collapse commences subsequently, with the net air mass transfer to the larynx, satisfying conservation of mass, since the larynx is considerably stiffer than the trachea. Collapse is gradual with increases in depth causing a corresponding decrease in luminal area (and hence volume, assuming constant length). The rate of change of reduction in luminal area is greater in early depth increases (871-950 m) than at later depths, and is evident through varying slope values in the graph of depth versus luminal area (Fig. 5). At the deepest depth of 1,280 m so far recorded (Doyle et al., 2008) the luminal area is estimated to be approximately 337 mm^2, which

represents a 41% decrease. The percentage volume change in the trachea from its initial compression at 871 m to the maximum depth analysed in this study at 1,500 m is very small representing just under 0.5% of the overall volume change in the system. The impact of gas compression at depth is therefore unlikely to contribute significantly to the leatherback's buoyancy state, in contrast to hard-shelled marine turtles (Hays, 2004).

In order to gain a visual representation of the extent of deformation of the trachea a two dimensional FE structural model of the trachea and adjacent soft tissues in the neck was created. The accuracy of the FE model in reproducing the volumetric changes predicted was measured through the calculation of the tracheal luminal area. For each increment of depth the luminal areas were evaluated and compared with the theoretical areas (Table 1). There is excellent agreement between these comparisons and between the two depth-luminal area relationships plotted in Fig. 5, confirming that the FE model succeeded in reproducing those areas computed through Boyle's law. For the depth of 1,280 m the area computed by the FE model was 340 mm^2, which correlates well with the theoretical value. Overall, the results from the FE model reveal the ability of the trachea to withstand the colossal hydrostatic pressures at depth and its extraordinary capability to collapse accordingly. Progressive re-inflation during ascent also facilitates the return of air mass to the lungs. Complete v-shaped dive profiles of two adult leatherbacks to 1,186 m (Fig. 1 in López-Mendilaharsu et al., 2009) and 1,250 m (Fig. 4C in Houghton et al., 2008) reveal that changes occur in both the rates of descent and ascent. In the case of the dive to 1,250 m there is a noticeable decrease in the rate of descent at approximately 750 m. This depth is similar to the depth predicted in this study (allowing for variations in turtle size and the assumptions made in this study) at which the lungs are expected to collapse completely and may be representative of descent rate alterations due to the cessation of air mass flow from the lungs. By applying the same collapse depth of 871 m predicted in this study (for a turtle with a curved carapace length of 168 cm, Davenport et al., 2009b) the lungs would be expected to be completely collapse for 19 minutes in the dive to 1,250 m and 22 minutes in the dive to 1,186 m. Essentially, it appears that the tracheal structure is perfectly suited for repeated collapse and re-inflation

The structural configuration of the leatherback trachea differs from the tracheae of other air-breathing vertebrates studied so far. In terrestrial mammals the trachea is generally composed of a series of horseshoe 'c-shaped' cartilaginous rings with flexible connective tissue between successive rings and smooth muscle tissue linking the tips of the rings (Wheater et al., 1979). This structural arrangement is different from deep-diving air-breathing oceanic mammals and reptiles such as dolphins, seals, whales and turtles. In these forms

tracheae differ noticeably through the irregular shape of the cartilaginous rings, that are sometimes complete (o-shaped); they also have reduced amounts of connective tissue and lack muscle tissue (Tarasoff and Kooyman, 1973; Davenport et al., 2009b; Bagnoli et al., 2011). Studies examining reductions in human tracheal volume have shown that decreases are achieved through inward movement of the smooth muscle connecting the two tracheal tips (Griscom and Wohl, 1983; Lindholm and Nyrén, 2005; Fitz-Clarke, 2007). In a similar manner, increases in volume are managed through outward protruding of the smooth muscle. A recent study on the behaviour of the trachea-bronchial tree of the bottlenose dolphin (*Tursiops truncatus*) showed that the extent of its collapse was much less when compared with that of a goat (*Capra aegagrus*; whose geometrical configuration is similar to that of Man) under the same loading conditions and at the same depths (Bagnoli et al., 2011). The difference was credited to the geometric arrangements of the dolphin trachea in which there was a much greater stiffness. It appears that the structural compositions of oceanic tracheae are superior structures for enduring collapse by comparison with their terrestrial relatives. The leatherback trachea confers both homogeneity and strength and, combined with the stabilising effect of the surrounding soft tissues, appears perfectly designed for collapse. Most terrestrial tracheae are poor designs for diving due to premature collapse of the cartilaginous rings and inward movement of the connecting smooth muscle tissue towards the ventral aspect. The geometry of the incomplete 'c-shaped' rings also implies that the stiffness distribution will not be uniform with a higher stiffness in the thicker central region than at the two tips. This configuration does not correlate well with withstanding the colossal pressures endured during repeated deep diving. In contrast to this, the particular geometry of the cartilage of *Dermochelys*, based on the o-shaped tracheal rings of reptiles, but with minimal connective tissue, appears to be advantageous for diving. The near elliptical shape (it is thicker ventrally than dorsally) actually promotes collapse and ensures a more uniform stress distribution in extreme bending states. Although deep dives are rare, the leatherback undertakes great numbers of dives each year. There are therefore appreciable numbers of dives to very deep depths with extreme pressure environments. The fact that the turtle is able to perform these dives regularly suggests that the collapse mechanism of the trachea may be optimised in order to successfully undertake repeated dives. In the simplified application of Boyle's law presented in this paper air mass flow from the collapsing lungs and alveoli in the early stages of the dive, promotes progressive collapse of the lungs and maintans the tracheal geometry. Subsequent tracheal collapse is also progresive, with the entrapped air acting as a counterbalance to the hydrostatic pressures and resisting premature deformation. The near-

elastic rubber-like behaviour of the cartilage facilitates progressive dilation during ascent allowing the air mass to flow gradually back into the lungs and alveoli at shallower depths. The findings of this study also demonstrate that the bulk of aerobic dives to depths shallower than 300-400 m will involve minimal distortion of the trachea despite the rubbery nature of its uncalcified walls. Our calculations indicate that it will remain inflated by air displaced from the lungs; it is not necessary to invoke a rigid trachea if the diver inhales before diving.

The noted rubber-like behaviour of the tracheal cartilage was modelled successfully by applying the Mooney-Rivlin formulation. Using the two calculated material constants the characteristic stress-strain relationship was established (Fig. 4). The relationship suggests that the material displays higher stiffness in compression than in tension, as evidenced by the greater slope in compression. As the Mooney-Rivlin formulation is a nonlinear hyper-elastic material model, stiffness increases with increments in strain. It is therefore not possible to make direct comparisons with many stiffness values for tracheal cartilage cited in the literature as a large proportion of these are based on linear elastic material behaviour. However, it may be seen from Fig. 4 that in tension the stress-strain relationship obtained in this study is approximately linear, yielding a stiffness value of 22.2MPa. This is slightly higher than published values and suggests that leatherback tracheal cartilage is a stiffer material. For example, a tensile Young's modulus value of 13.389±4.230 MPa, was recorded in experimental research on striped dolphins (*Stenella coeruleoalba*; Cozzi et al., 2005). Other estimates of Young's modulus from biomechanical tensile testing of human tracheal rings range from 13.6±1.5 MPa in the ablumenal superficial zone to 4.6±1.7MPa in the central area (Roberts et al., 1997). Further studies on human tracheal cartilage used or obtained stiffness values that were of the magnitude of 3.33 MPa (Trabelsi et al., 2010), 2.5-7.7 MPa (Lambert et al., 1991), 16.67 MPa (Begis et al., 1988) and 10 MPa (Holzhäuser and Lambert, 2001). Maturity and location have also been determined to be factors affecting stiffness with the age of samples, between 1.8±2.1 MPa-15±5.1 MPa (Rains et al., 1992), and depth, between 1-20 MPa (Roberts et al., 1997), showing large variations. Studies on terrestrial vertebrate tracheae have recorded values of 5.364±1.591 MPa and 3.735±1.433 MPa in goats and pigs respectively (Cozzi et al., 2005). It appears that the characteristic material properties may be species, age and location dependant. In this paper the material properties were obtained by fitting a rubber material model to experimental data obtained from the compressive testing of a leatherback tracheal portion. This simulates the real nonlinear behaviour of the material. The indication of higher stiffness in compression than in tension agrees with findings in other studies (Teng et al., 2008; Teng et al., 2009a; Teng et

al., 2009b). More appropriate material models for cartilage are a current area of research. Another area of potential study lies in the tracheae of those diving vertebrates that apparently have stiffer tracheae by virtue of calcification of the tracheal rings (e.g. sea otters).

Some limitations could not be avoided when undertaking this study. As mentioned earlier certain assumptions were made in the application of Boyle's law regarding the response of the respiratory system. In particular, changes in length in both the trachea and larynx, as well as reductions in lung volume due to the increasing partial pressures of all air gases during descent were neglected. Assumptions were also made with regards to the constitutive material model used to model tracheal cartilage material behaviour. Collagen type II, which is one of the primary constituents of tracheal cartilage has been shown to be a highly nonlinear material (Sun et al., 2004). It is, therefore, rational to expect that tracheal cartilage should also exhibit nonlinear behaviour, and this has been suggested in studies using mathematical models based on simple beam bending theory (Teng et al., 2008; Teng et al., 2009a; Teng et al., 2009b). In the past tracheal cartilage has also been treated as a linear elastic material in studies using three dimensional FE analyses (Begis et al., 1988; Costantino et al., 2004) and mathematical models based on thin curved beam theory (Lambert et al., 1991) and on the physics of a shell (Holzhäuser and Lambert, 2001). Additionally, linear elastic properties have been assumed in experimental material studies (Rains et al., 1992; Cozzi et al., 2005) as has hyper-elasticity (Teng et al., 2008; Teng et al., 2009a; Teng et al., 2009b; Trabelsi et al., 2010). The results from our material testing show that the load-displacement history is approximately linear during loading (Fig. 3). If the sample being tested also had uniform thickness the stress-strain relationship would also be expected to be linear. This may explain why the material has been treated as linear elastic in previous studies. In order to investigate the rubber–like behaviour of the tracheal samples studied here the tracheal cartilage was analysed using the Mooney-Rivlin hyperelastic material model, the material constants of which were obtained from compressive experimental testings.

This study aspired to investigate the response of the trachea of the leatherback turtle in the extreme pressure environments it is subjected to during deep diving using a simplified application of Boyle's law and a corresponding FE model. The results produced both mathematically, and from the FE model itself, reveal that the trachea collapses and dilates progressively with variations in depth. It appears to be a superior structure for managing collapse when compared with the tracheae of terrestrial vertebrates and the tracheae of shallow divers (including humans). Complete (o-shaped) rings and the lack of connective tissue provide an almost solid elliptical tube structure that, when combined with air mass

flow from the lungs, faciliates progressive deformation. Indeed, the struture appears perfectly designed to promote recoverable collapse. The results from this study should benefit further research on the response of biological soft tissues in extreme pressure environments.

Acknowledgements

The authors are grateful to Dr Tom Doyle and Mr Luke Harman for collection of the leatherback turtle material. They also thank Ms Tracy Cuffe for technical assistance and Dr Paddy McLaughlin for help with preparation of CT scans.

Funding

This study was funded by the Irish Research Council for Science, Engineering and Technology (IRCSET) through their 'EMBARK' initiative and by the John Sisk Postgraduate Research Scholarship in Civil Engineering at University College Cork. The support received from both sources is graciously acknowledged.

LIST OF SYMBOLS/ABBREVIATIONS USED

DCS	decompression sickness
mya	million years ago
FE	finite element
2-D	two-dimensional
LG	lung
T	trachea
LX	larynx
P	pressure acting on system
x	depth
V	volume of system
k	Boyle's constant
V_{LGx}	volume of lungs at depth x
P_0	initial pressure at surface level
P_X	pressure at depth x
V_{LX0}	volume of larynx at surface level
V_{T0}	volume of trachea at surface level
V_{LG0}	volume of lungs at surface level
V_{LXx}	volume of larynx at depth x
V_{Tx}	volume of trachea at depth x
ρ	density
g	acceleration due to gravity
P_{ATM}	atmospheric pressure

REFERENCES

Bagnoli, P., Cozzi, B., Zaffora, A., Acocella, F., Fumero, R. and Laura Costantino, M. (2011). Experimental and computational biomechanical characterisation of the tracheo-bronchial tree of the bottlenose dolphin (*Tursiops truncatus*) during diving. *J. Biomech.* **44**, 1040-1045.

Begis, D., Delpuech, C., Le Tallec, P., Loth, L., Thiriet, M. and Vidrascu, M. (1988). A finite-element model of tracheal collapse. *J. Appl. Physiol.* **64**, 1359-1368.

Bostrom, B. L., Fahlman, A. and Jones, D. R. (2008). Tracheal compression delays alveolar collapse during deep diving in marine mammals. *Resp. Physiol. Neurobiol.* **161**, 298-305.

Costantino, M. L., Bagnoli, P., Dini, G., Fiore, G. B., Soncini, M., Corno, C., Acocella, F. and Colombi, R. (2004). A numerical and experimental study of compliance and collapsibility of preterm lamb tracheae. *J. Biomech.* **37**, 1837-1847.

Cozzi, B., Bagnoli, P., Acocella, F. and Costantino, M. L. (2005). Structure and biomechanical properties of the trachea of the striped dolphin *Stenella coeruleoalba*: evidence for evolutionary adaptations to diving. *Anat. Rec.* **284A**, 500-510.

Davenport, J., Fraher, J., Fitzgerald, E., McLaughlin, P., Doyle, T., Harman, L. and Cuffe, T. (2009a). Fat head: an analysis of head and neck insulation in the leatherback turtle (Dermochelys coriacea). *J. Exp. Biol.* **212**, 2753-2759.

Davenport, J., Fraher, J., Fitzgerald, E., McLaughlin, P., Doyle, T., Harman, L., Cuffe, T. and Dockery, P. (2009b). Ontogenetic changes in tracheal structure facilitate deep dives and cold water foraging in adult leatherback sea turtles. *J. Exp. Biol.* **212**, 3440-3447.

Davenport, J., Plot, V., Georges, J. Y., Doyle, T. K. and James, M. C. (2011). Pleated turtle escapes the box–shape changes in *Dermochelys coriacea*. *J. Exp. Biol.* **214**, 3474-3479.

Doyle, T. K., Houghton, J. D. R., O'Súilleabháin, P. F., Hobson, V. J., Marnell, F., Davenport, J. and Hays, G. C. (2008). Leatherback turtles satellite-tagged in European waters. *Endangered Spec. Res.* **4**, 23-31.

Eckert, K. L. and Luginbuhl, C. (1988). Death of a giant. *Mar. Turtle Newsl.* **43**, 1-3.

Eckert, S. A., Eckert, K. L., Ponganis, P. and Kooyman, G. L. (1989). Diving and foraging behaviour of leatherback sea turtles (*Dermochelys coriacea*). *Can. J. Zool.* **67**, 2834-2840.

Eckert, S. A., Nellis, D. W., Eckert, K. L. and Kooyman, G. L. (1986). Diving patterns of two leatherback sea turtles (*Dermochelys coriacea*) during internesting intervals at Sandy Point, St. Croix, US Virgin Islands. *Herpetologica* **42**, 381-388.

Fitz-Clarke, J. R. (2007). Mechanics of airway and alveolar collapse in human breath-hold diving. *Resp. Physiol. Neurobiol.* **159**, 202-210.

Fossette, S., Gleiss, A. C., Myers, A. E., Garner, S., Liebsch, N., Whitney, N. M., Hays, G. C., Wilson, R. P. and Lutcavage, M. E. (2010). Behaviour and buoyancy regulation in the deepest-diving reptile: the leatherback turtle. *J. Exp. Biol.* **213**, 4074-4083.

Fraher, J., Davenport, J., Fitzgerald, E., McLaughlin, P., Doyle, T., Harman, L. and Cuffe, T. (2010). Opening and closing mechanisms of the leatherback sea turtle larynx: a crucial role for the tongue. *J. Exp. Biol.* **213**, 4137-4145.

Fung, Y. C. (1993). Biomechanics - Mechanical Properties of Living Tissue. Berlin: Springer-Verlag.

Griscom, N. T. and Wohl, M. E. (1983). Tracheal size and shape: effects of change in intraluminal pressure. *Radiology* **149**, 27-30.

Hays, G. C., Metcalfe, J. D., Walne, A. W. (2004). The implications of lung-regulated bioyancy control for dive depth and duration. *Ecology* **85**, 1137-1145.

Holzhäuser, U. and Lambert, R. K. (2001). Analysis of tracheal mechanics and applications. *J. Appl. Physiol.* **91**, 290-297.

Hooker, S. K., Fahlman, A., Moore, M. J., Aguilar de Soto, N., de Quirós, Y. B., Brubakk, A. O., Costa, D. P., Costidis, A. M., Dennison, S., Falke, K. J. et al. (2011). Deadly diving? Physiological

and behavioural management of decompression stress in diving mammals. *Proc. R. Soc. Lond. B. Biol. Sci.*, doi:10.1098/rspb.2011.2088 Published online.

Houghton, J. D. R., Doyle, T. K., Davenport, J., Wilson, R. P. and Hays, G. C. (2008). The role of infrequent and extraordinary deep dives in leatherback turtles (*Dermochelys coriacea*). *J. Exp. Biol.* **211**, 2566-2575.

Kooyman, G. L. (1989). Diverse Divers: Physiology and Behaviour. Berlin, Heidelberg, New York: Springer-Verlag.

Kooyman, G. L., Hammond, D. D. and Schroeder, J. P. (1970). Bronchograms and tracheograms of seals under pressure. *Science* **169**, 82-84.

Kooyman, G. L. and Sinnett, E. E. (1982). Pulmonary shunts in harbor seals and sea lions during simulated dives to depth. *Physiol. Zool.* **55**, 105-111.

Lambert, R., Baile, E., Moreno, R., Bert, J. and Pare, P. (1991). A method for estimating the Young's modulus of complete tracheal cartilage rings. *J. Appl. Physiol.* **70**, 1152-1159.

LeBoeuf, B. J., Costa, D. P., Huntley, A. C., Kooyman, G. L. and Davis, R. W. (1986). Pattern and depth of dives in northern elephant seals, *Mirounga angustirostris*. *J. Zool. Lond.* **208**, 1-7.

Lindholm, P. and Nyrén, S. (2005). Studies on inspiratory and expiratory glossopharyngeal breathing in breath-hold divers employing magnetic resonance imaging and spirometry. *Eur. J. Appl. Physiol.* **94**, 646-651.

López-Mendilaharsu, M., Rocha, C. F. D., Domingo, A., Wallace, B. P. and Miller, P. (2009). Prolonged deep dives by the leatherback turtle *Dermochelys coriacea*: pushing their aerobic dive limits. *JMBA2 Biodiversity Records* **6274 (on-line)**.

Lutcavage, M. E., Bushnell, P. G. and Jones, D. R. (1992). Oxygen stores and aerobic metabolism in the leatherback sea turtle. *Can. J. Zool.* **70**, 348-351.

Miller, P. J. O., Johnson, M. P., Tyack, P. L. and Terray, E. A. (2004). Swimming gaits, passive drag and buoyancy of diving sperm whales *Physeter macrocephalus*. *J. Exp. Biol.* **207**, 1953-1967.

Moore, C., Fahlman, A., Moore, M., Niemeyer, M., Lentell, B., Oakes, S. and Trumble, S. (2011a). Histological investigation of the "slip" in marine mammal tracheas. Conference Paper. Society for Marine Mammology. 19th Biennial conference on the biology of Marine Mammals. Tampa, Florida, November 27 - December 2, 2011.

Moore, M. J., Hammar, T., Arruda, J., Cramer, S., Dennison, S., Montie, E. and Fahlman, A. (2011b). Hyperbaric computed tomographic measurement of lung compression in seals and dolphins. *J. Exp. Biol.* **214**, 2390-2397.

Murphy, C., Kelliher, D. and Davenport, J. 2010. A nonlinear finite element inverse approach to characterise the material properties of tracheal cartilage: Preliminary study. Proceedings of the ASME 2010 Summer Bioengineering Conference. Naples, Florida, June 16 - 19, 2010.

Ponganis, P. J., Kooyman, G. L. and Castellini, M. A. (1993). Determinants of the aerobic dive limit of Weddell seals: analysis of diving metabolic rates, postdive end tidal pO_2's, and blood and muscle oxygen stores. *Physiol. Zool.* **66**, 732-749.

Rains, J., Bert, J., Roberts, C. and Pare, P. (1992). Mechanical properties of human tracheal cartilage. *J. Appl. Physiol.* **72**, 219-225.

Roberts, C. R., Rains, J. K., Paré, P. D., Walker, D. C., Wiggs, B. and Bert, J. L. (1997). Ultrastructure and tensile properties of human tracheal cartilage. *J. Biomech.* **31**, 81-86.

Sato, K., Mitani, Y., Cameron, M. F., Siniff, D. B. and Naito, Y. (2003). Factors affecting stroking patterns and body angle in diving Weddell seals under natural conditions. *J. Exp. Biol.* **206**, 1461-1470.

Sato, K., Naito, Y., Kato, A., Niizuma, Y., Watanuki, Y., Charrassin, J., Bost, C. A., Handrich, Y. and Le Maho, Y. (2002). Buoyancy and maximal diving depth in penguins: do they control inhaling air volume? *J. Exp. Biol.* **205**, 1189-1197.

Scholander, P. F. (1940). Experimental investigations on the respiratory function in diving mammals and birds. *Hvalradets Skrifter* **22**, 1-131.

Spotila, J. R. (2004). Sea turtles: A Complete Guide To Their Biology, Behavior, And Conservation. 240 pp. Baltimore: Johns Hopkins University Press.

Sun, Y. L., Luo, Z. P., Fertala, A. and An, K. N. (2004). Stretching type II collagen with optical tweezers. *J. Biomech.* **37**, 1665-1669.

Tarasoff, F. and Kooyman, G. (1973). Observations on the anatomy of the respiratory system of the river otter, sea otter, and harp seal. I. The topography, weight, and measurements of the lungs. *Can. J. Zool.* **51**, 163-170.

Teng, Z., Ochoa, I., Li, Z. and Doblare, M. (2009a). Study of tracheal collapsibility, compliance and stress by considering its asymmetric geometry. *Med. Eng. Phys.* **31**, 328-336.

Teng, Z., Ochoa, I., Li, Z., Liao, Z., Lin, Y. and Doblare, M. (2009b). Study on Tracheal Collapsibility, Compliance, and Stress by Considering Nonlinear Mechanical Property of Cartilage. *Ann. Biomed. Eng.* **37**, 2380-2389.

Teng, Z., Ochoa, I., Li, Z., Lin, Y., Rodriguez, J. F., Bea, J. A. and Doblare, M. (2008). Nonlinear mechanical property of tracheal cartilage: A theoretical and experimental study. *J. Biomech.* **41**, 1995-2002.

Trabelsi, O., del Palomar, A. P., López-villalobos, J. L., Ginel, A. and Doblaré, M. (2010). Experimental characterization and constitutive modeling of the mechanical behavior of the human trachea. *Med. Eng. Phys.* **32**, 76-82.

Wheater, P. R., George Burkitt, H. and Daniels, V. G. (1979). Functional Histology-A Text and Colour Atlas. Edinburgh, London and New York: Churchill Livingstone.

Wood, R. C., Johnson-Gove, J., Gaffney, E. S. and Maley, K. F. (1996). Evolution and phylogeny of the leatherback turtles (Dermochelyidae), with descriptions of new fossil taxa. *Chelion Conserv. Bi.* **2**, 266-286.

FIGURE LEGEND

Fig. 1 **A** Material testing setup

B Close- up of material during compressive testing

Fig. 2 FE model setup of leatherback neck showing location of vertebral column and tracheal luminal area. Network of lines represents fine mesh required for FE analyses. Soft tissues and trachea denoted by blue and orange respectively. (For interpretation of the references to colour in this figure legend, the reader is referred to the web version of this article.)

Fig. 3 Complete load-displacement history obtained from the compressive material testing of an adult leatherback cartilaginous ring. Six continuous loading and unloading cycles were recorded and are shown in ascending numeric order through the blue, green, orange, red, purple and black lines respectively. (For interpretation of the references to colour in this figure legend, the reader is referred to the web version of this article.)

Fig. 4 Stress-strain relationship obtained from the compressive testing of the leatherback tracheal cartilage in this study using the Mooney-Rivlin formulation

Fig. 5 Leatherback respiratory system (lungs, trachea and larynx) volume-depth and tracheal luminal area-depth relationships with FE luminal area deformations at selected increments of depth. Blue lines represent collapse calculated using the simplified application of Boyle's law (Eqn 2, Eqn 3) and using lung volume estimates made by Lutcavage et al. (1992). The red line represents collapse computed from the FE model results. (For interpretation of the references to colour in this figure legend, the reader is referred to the web version of this article)

Fig. 1

(a)

(b)

Fig. 2

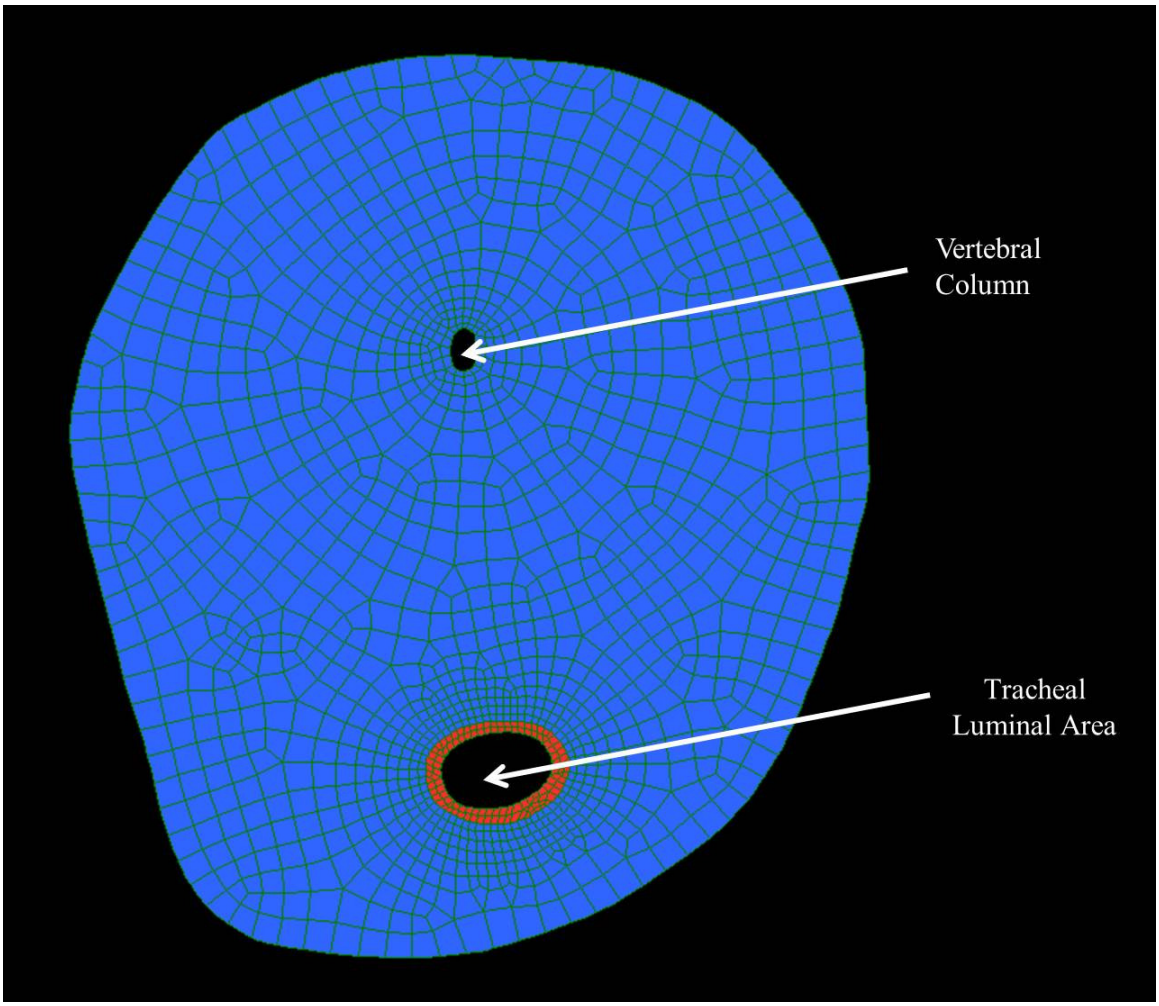

Fig. 3

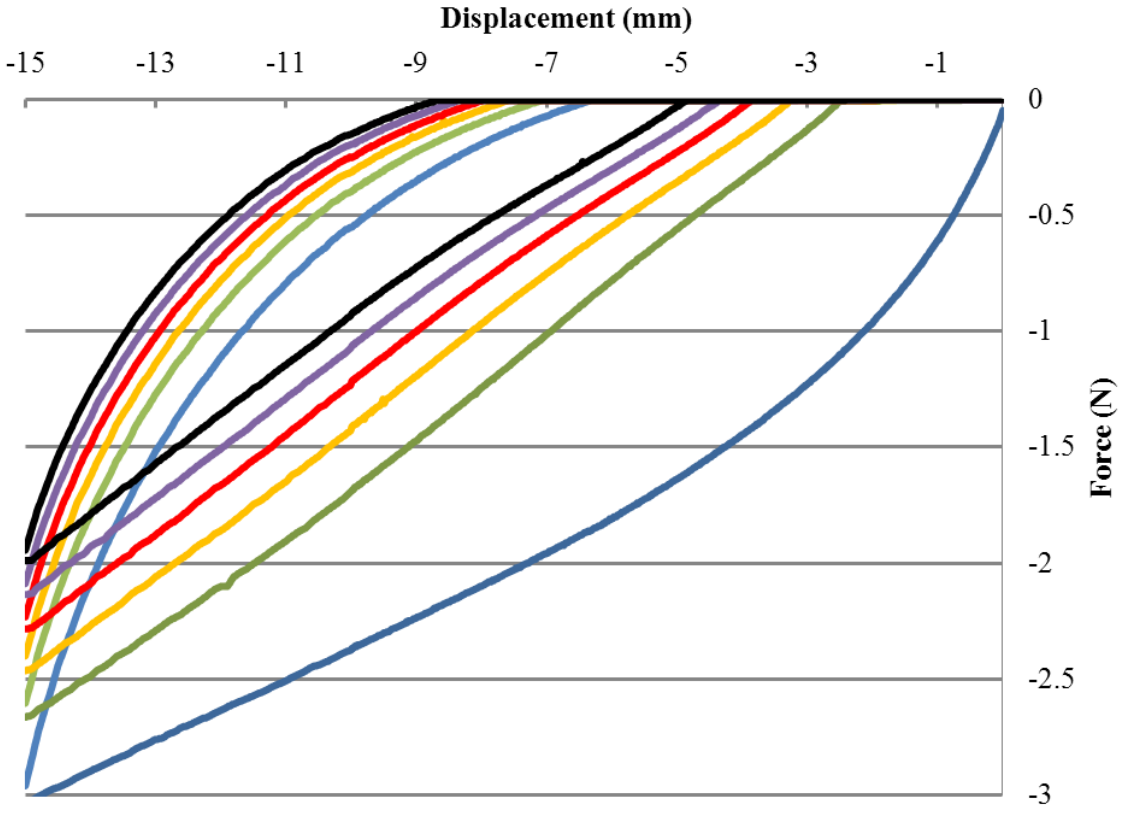

Fig. 4

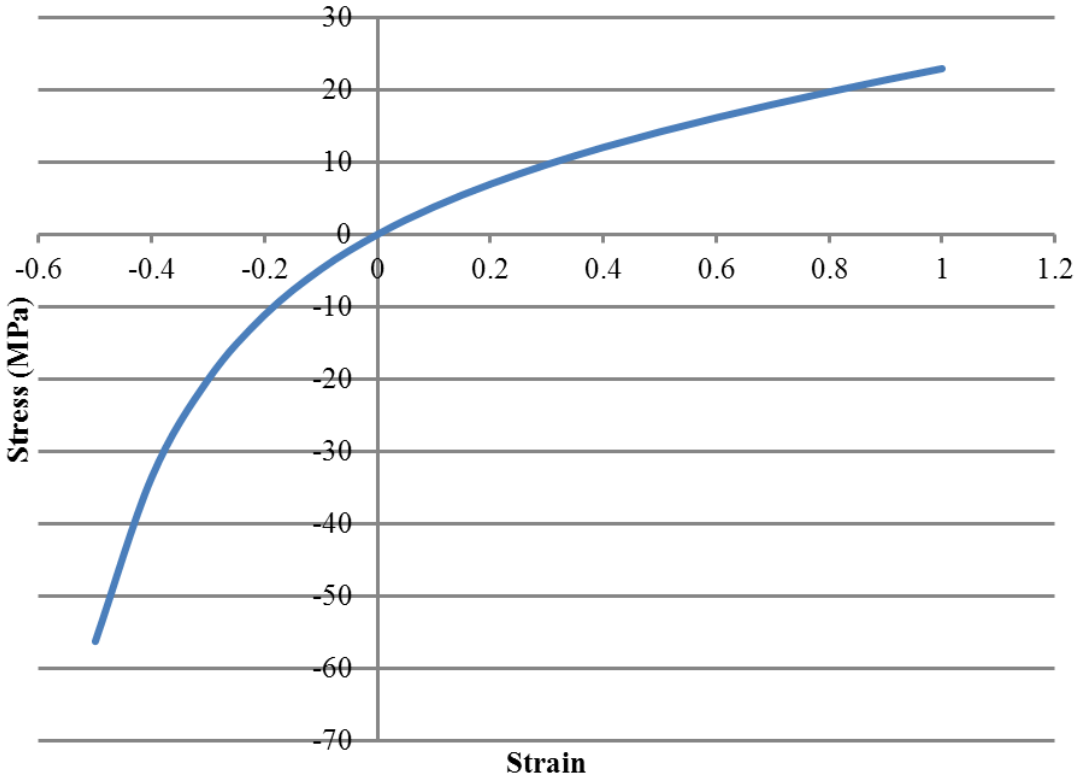

Fig. 5

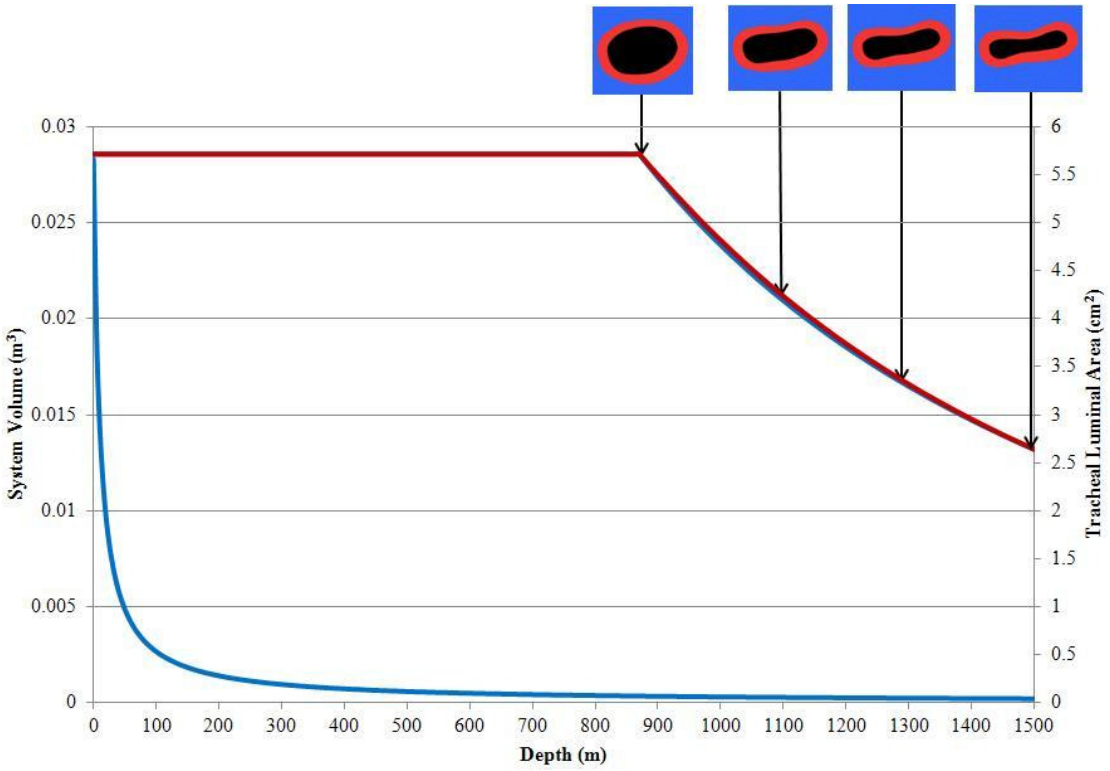

TABLE LEGEND

Table 1 Comparison of tracheal luminal areas calculated using simplified application of Boyle's law with corresponding area computed from FE model results

Table 1

Depth (m)	Idealised Boyle's law (mm^2)	FE model results (mm^2)
875	568	568
900	548	550
950	511	515
1000	477	482
1050	447	452
1100	419	424
1150	394	398
1200	371	374
1250	349	352
1300	330	332
1350	311	313
1400	294	295
1450	279	279
1500	264	264

EQUATION LEGEND

Eqn 1

$$PV = k$$

P = pressure

V = volume

k = Boyle's constant

Eqn 2

$$V_{LGx} = \frac{P_0}{P_x}\left(V_{LX0} + V_{T0} + V_{LG0}\right) - V_{LXx} - V_{Tx},$$

x = depth

V_{LGx} = volume of the lungs at depth x

P_0 = initial pressure at surface level

P_x = pressure at depth x

V_{LX0} = volume of the larynx at surface level

V_{T0} = volume of the trachea at surface level

V_{LG0} = volume of the lungs at surface level

V_{LXx} = volume of the larynx at depth x

V_{Tx} = volume of the trachea at depth x

Eqn 3

$$V_{Tx} = \frac{P_0}{P_x}\left(V_{LX0} + V_{T0} + V_{LG0}\right) - V_{LXx}$$

x = depth

V_{Tx} = volume of the trachea at depth x

P_0 = initial pressure at surface level

P_x = pressure at depth x

V_{LX0} = volume of the larynx at surface level

V_{T0} = volume of the trachea at surface level

V_{LG0} = volume of the lungs at surface level

V_{LXx} = volume of the larynx at depth x